Catalysis Today 174 (2011) 141–147

Contents lists available at ScienceDirect

Catalysis Today

journal homepage: www.elsevier.com/locate/cattod

Photocatalytic NO reduction with C_3H_8 using a monolith photoreactor

Yi-Hui Yu, Yung-Tin Pan, Yi-Ting Wu, Janusz Lasek, Jeffrey C.S. Wu*

Department of Chemical Engineering, National Taiwan University, No. 1 Section 4 Roosevelt Road, Taipei 10617 Taiwan

ARTICLE INFO

Article history:
Received 26 October 2010
Received in revised form 14 January 2011
Accepted 18 January 2011
Available online 16 February 2011

Keywords:
NO
Photoreduction
Photocatalysis
Monolithic photoreactor

ABSTRACT

Photocatalytic reduction of nitric oxide was studied on a PtO_xPdO_y/TiO_2-coated monolith photoreactor using propane as the reducing agent. The performance of NO reduction was compared under three reaction conditions including NO/propane, NO/propane/O_2 and NO/propane/H_2O at three reaction temperatures, 25, 70 and 120 °C. The NO/propane system showed the best performance of near 90% conversion at 25 °C. The NO conversion decreased slightly as temperature increased in NO/propane system, however, NO/propane/O_2 and NO/propane/H_2O systems showed an opposite trend. Oxygen and water significantly inhibited the reduction of NO because oxygen competed with NO as oxidant, and water interfered the adsorption of both NO and propane. TiO_2 became super-hydrophilic under UV-light irradiation thus the catalyst surface was easily covered by water in moisture condition. By increasing the reaction temperature, water tended to desorb from the catalyst surface thus released more active sites for NO photoreduction. An in situ FTIR was also performed to study the intermediate species of the NO/propane and NO/propane/O_2 systems under UV-light irradiation. The results indicated that NO went through both oxidation and reduction with C_3H_8 on PtO_xPdO_y/TiO_2. The reaction path of NO might change with increasing temperature.

1. Introduction

Nowadays Earth is facing numerous environmental problems mainly due to the massive amount of pollutants produced by industrial and transportation activities. One of the air pollutants, nitrogen oxides (NO_x), which emitted from stationary thermal power plants and internal combustion engines of transportation facilities are the main hazardous atmospheric pollutants responsible for the acid rain formation, photochemical smog. Nitric oxide (NO) also plays a role in ozone layer depletion. Research of converting NO_x to nitrogen has been extensively studied for a long period of time, and a number of processes have already been industrialized [1,2]. For example, the selective catalytic reduction (SCR) process is a method currently used in de-NO_x for stationary and mobile sources. However, these conventional processes need to operate at high temperatures, which result in a comparatively high cost. Therefore, the low-temperature photocatalytic degradation of NO_x becomes an appealing alternative for energy saving purposes. Furthermore, sunlight is possible to be used for this photo-driven reaction.

Titanium dioxide (TiO_2) is a common photocatalyst in numerous researches due to its high reactivity under light irradiation, stable in storage, non toxicity, and low cost [3–5]. A great amount of researches were focused on the gas phase heterogeneous photocatalytic reaction, especially for air pollution treatments. In view of the traditional SCR, ammonia (NH_3) and carbon monoxide (CO) were used as the reductants for the reduction of NO in the photo-SCR system [6–10]. Although NH_3 and CO showed good selectivity towards complete reduction of NO to N_2 under light irradiation, the corrosive or toxic nature makes them unfavorable for environmental applications. Other than NH_3 or CO, hydrocarbons also served as reductants in the traditional selective catalytic reduction, denoted as HC-SCR, because hydrocarbons existed in the flue gas [1,2,11,12]. Moreover, hydrocarbons are relatively much stable and safer than NH_3 and CO. The researches of photocatalytic oxidization (PCO) of volatile hydrocarbons, such as propane [13,14] and propylene [15], showed that light hydrocarbons could be easily oxidized on the TiO_2 surface. Thus coupling the PCO of light-hydrocarbons with photocatalytic reduction of NO is excellent choice. However, little research on the photocatalytic reduction of NO_x by hydrocarbons has been reported so far.

The reaction temperature plays an important role to photocatalytic reduction of NO. Zhang et al. reported a good performance of 10 ppm NO reduction under room temperature [5]. Lim et al. showed that the NO conversion increases with temperature in a fluidized-bed reactor [16]. Poulston proposed that NO underwent reduction at higher temperature as 150 °C while NO was oxidized at ambient temperature in hydrocarbon environments [17]. From the above literatures, the variation of temperature substantially influences the performance of NO reduction/oxidation but the detail relations are still unclear.

* Corresponding author. Tel.: +886 23631994; fax: +886 23623040.
E-mail address: cswu@ntu.edu.tw (J.C.S. Wu).

0920-5861/$ – see front matter © 2011 Elsevier B.V. All rights reserved.
doi:10.1016/j.cattod.2011.01.024

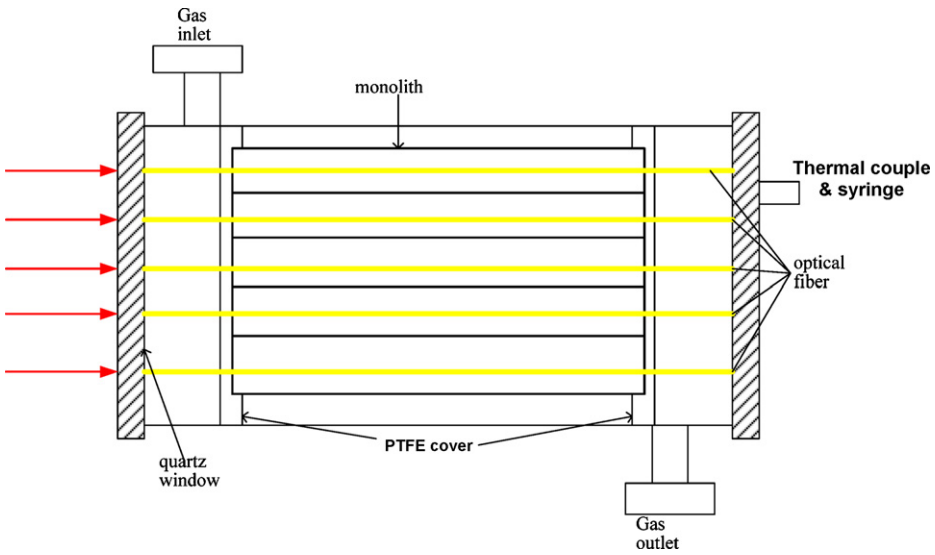

Fig. 1. The schematics of the monolith photoreactor.

Most of the researches focus on two sides of photocatalysis. One is photocatalysts, and reaction engineering is the other. Literature has shown that loading platinum (Pt) or palladium (Pd) metal on the surface of TiO_2 could improve its photocatalytic performance [18,19]. Several reactor design for photocatalysis were established [20], such as the packed bed reactor and optical fiber reactor. The monolith is widely used in industrial process due to the advantage of low-pressure drop and high surface-to-volume ratio, which are very suitable for gas-solid reaction. The use of monolith for the photocatalytic reactions has been studied by several research groups [21–25]. Although monolith has many advantages, one of the major drawbacks is its poor performance on photocatalytic reactions due to poor illumination of internal channels. Studies show that in side illumination systems, a fraction of the photon flux would be blocked outside the channels and the light intensity decays rapidly along the monolith channel, leaving only a small portion of the monolith channels being illuminated [26–29]. Ren and Valsaraj [30] and Mul's group [24,25] had proposed a novel design inserting optical fibers into the monolith channels. By doing so, the distance of illumination in the monolith channels can be effectively prolonged and as a consequent, higher quantum efficiency for the photoreduction of pollutants can be achieved.

In the present study, photocatalytic reduction of NO by propane as was investigated using a photocatalyst-coated monolith photoreactor. The influences of oxygen and water on NO conversion at various reaction temperatures were studied in three reaction conditions, NO/propane, NO/propane/O_2 and NO/propane/H_2O. An in situ FTIR experiment was also performed to reveal the surface species formed during the reaction at various reaction temperatures, and to explore the possible reaction mechanism.

2. Experimental

2.1. Preparation and characterization of catalysts

The preparation of the PtO_xPdO_y/TiO_2 thin film was in two parts, which were the synthesis of TiO_2 photocatalyst sol by controlled thermal hydrolysis of tetrabutoxide titanate (TBOT) and the metal loading process. For the synthesis of TiO_2, TBOT was added by droplets to a solution of 0.1 M nitric acid with a volume ratio of 1:6 (TBOT:nitric acid). After the solution was stirred and heated to 80 °C, polyethylene glycol (PEG) was added with half the weight of TiO_2, and the solution was maintained at this temperature, stirred for 8 h to complete the hydrolysis of TBOT. The loading metal precursors, $Pd(NO_3)_2$ and H_2PtCl_6, were added during the aging process with each of the amount of 1 wt% of the TiO_2. Four types catalysts, TiO_2, 1 wt% Pt/TiO_2, 1 wt% Pd/TiO_2, and 1 wt% Pt 1 wt% Pd/TiO_2 were synthesized.

The Corning monolith is composed by cordierite ($2Al_2O_3{\cdot}5SiO_2{\cdot}2MgO$, 30% porosity) which has 54 circular channels per square inch of its cross section. The dimension of the monolith is 4.2 cm in diameter and 6.0 cm in length. The monolith is relatively porous thus needs pretreatments to reduce its micropores in order to coat a thin film of catalyst on the internal channels. To achieve this target, dip-coating method was applied to form a pre-coated SiO_2 layer with a uniform mixture of SiO_2 precursor and PEG on the channel walls [31], which could fill in most micropores such that a smooth upper layer could be obtained for a uniform light irradiation. The silica sol was prepared by the catalyzed hydrolysis of tetraethyl orthosilicate (TEOS). After calcination at 500 °C, the SiO_2 layer was formed. The TiO_2 sol was dip-coated on top of SiO_2 sublayer then dried 3 h in air at 150 °C following by calcination at 500 °C for 5 h. A TiO_2 thin film with the amount of 0.41 g was obtained on the monolith.

The crystalline phases of TiO_2, PdO_y/TiO_2, PtO_x/TiO_2, and PtO_xPdO_y/TiO_2 were determined by X-ray diffraction (Rigaku-Ultima IV MAC Science) and the light absorption of photocatalysts was characterized by ultraviolet–visible light (UV–vis) spectroscopy (Varian, Cary 100).

2.2. Photoreaction system

Fig. 1 shows a schematic of the monolith photoreactor. The catalyst-coated monolith was inserted by side-glowed optical fiber in each channel and placed inside a circular quartz vessel. The PMMA side-glowed optical fiber with 0.5 mm diameter was manufactured by Hong Yi optical fibers company, Taiwan. Two PTFE cover-rings sealed both ends of the monolith so that the reactants only flowed through the channels from one end to the other. The reactor was irradiated from one side of quartz window so that the side-glowed optical fibers can illuminate the catalyst on the internal surface of the monolith channel during the reaction. The light source was provided by the Exfo S1500 (USA) equipped with a high-pressure Hg lamp and a guiding optical fiber with filter to emit UV-A light (320–500 nm) at the intensity of 46.9 mW/cm^2. The reaction temperature was maintained by a heating tape wrapped around

the quartz vessel and controlled by a thermal couple inserted in the central monolith channel. Another powder-form reactor was constructed with the same configuration as the monolith photoreactor except no monolith inside for comparison. A quartz plate, 4.5 cm × 10.5 cm, was placed inside the reactor and inclined an angle of 5–10° facing the irradiating UV light from the quartz window. The powder catalyst with the same composition and weight in the monolith was evenly spread on the quartz plate.

The composition of the feed was mixed two streams of NO (400 ppmv in N_2) and propane (C_3H_8 5000 ppmv in N_2) with the NO to propane ratio of 1:24. The total flow rate was kept at 7 ml/min equivalent to VHSV near 19 min by mixing additional pure N_2 stream. The reaction was carried out under UV irradiation for 4 h after steady-state flow was reached. The concentrations of NO and NO_2 were simultaneously measured by a chemiluminescenece NO_x analyzer (Teledyne Instruments, M200E). Additional oxygen was introduced with a third stream of 5% O_2 in helium and water vapor was attained by passing the propane stream through a water saturator at room temperature. The total flow rate was still maintained at 7 ml/min by adjusting additional pure N_2 stream. N_2O, which is one of the by-products, was measured every hour by a GC (Young Lin Instrument, Acme6100, Korea) equipped with TCD using Porapak Q column. The amount of N_2O was found negligible. Hydrocarbon intermediates in the gas phase were detected by the same GC in another channel equipped with FID using Porapak N column. When the reaction was over, the monolith was soaked in water to dissolve the nitrite and nitrate formed on the catalyst during the photoreaction. An ion chromatograph (EDIONEX, 2000i/SP) was used to measure the amount of nitrite and nitrate in aqueous solution. Nitrite and nitrate would not desorb to gas stream once they formed on the surface (see Section 3 and Fig. 12). We found less than 1% of nitrite and nitrate was formed from the NO photoreaction. Thus the N_2 selectivity was very closed the total amount of NO consumed, which was near 99%.

2.3. In situ FTIR spectroscopy

The photocatalytic reduction of NO was studied by in situ diffuse reflectance infrared Fourier transform spectroscopy (DRIFTS) on Nexus 470 IR spectrometer (Thermo Nicolet) equipped with a liquid N_2 cooled MCT detector. The photocatalyst, ~150 mg, was placed in a HVC dome reactor (HVC; Harrick HVC-DRP-1) with three windows, including two KBr windows and a quartz window [32]. The molar ratio of the gas mixture was the same as that for the reaction system. Photoreaction was performed in a closed reaction under UV irradiation through the quartz window for 19 min. The reaction temperature was controlled by a built-in heating tape. All spectra were measured with a resolution of 4 cm^{-1} and accumulating 64 scans. The spectrum was obtained by subtracting the background of fresh photocatalyst under Helium environment.

3. Results and discussion

Fig. 2 is the UV–vis spectra of the various powder-form catalyst. The spectrum of pure TiO_2 shows no absorbance in the visible light region. The PtO_x/TiO_2 has wide absorbance at the visible light region. The PdO_y/TiO_2 has an absorbance band around 400–500 nm. The PtO_xPdO_y/TiO_2 shows both characteristics of the shoulder at 400–500 nm and the strong absorbance at visible light region. From the XRD pattern in Fig. 3, all catalysts showed identical patterns of TiO_2 anatase phase. There were no related peaks shown the existence of PtO_x or PdO_y indicating that PtO_x or PdO_y clusters were uniformly dispersed on the catalyst surface. Based to the results of UV–vis and XRD, the PtO_xPdO_y/TiO_2 was successfully synthesized.

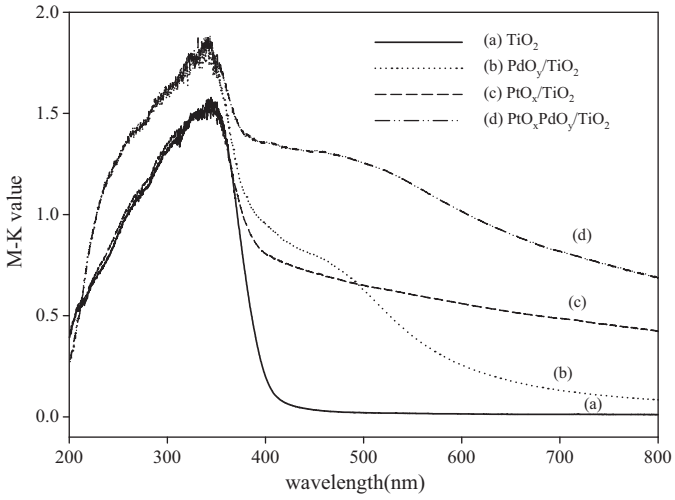

Fig. 2. UV–vis spectra of fresh catalysts.

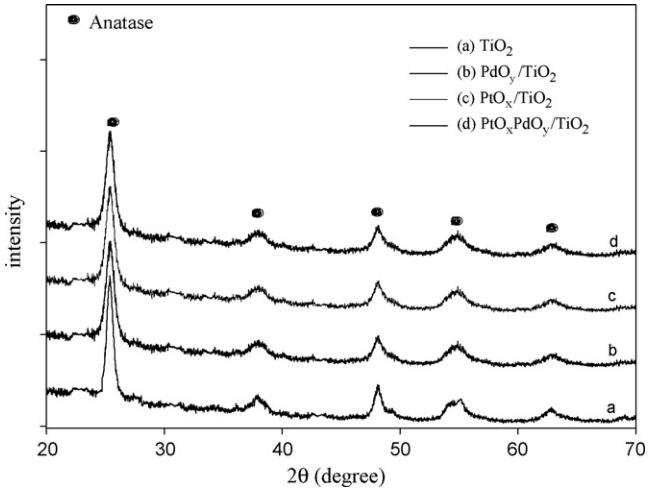

Fig. 3. XRD patterns of fresh catalysts.

Table 1 is the summary of the performance of NO conversion on four catalysts. The pure TiO_2 gave 60% conversion of NO. The conversions of PtO_x/TiO_2 and PdO_y/TiO_2 increased slightly while the conversion of PtO_xPdO_y/TiO_2 increased to 69.5%. Fig. 4 shows the instantaneous concentration of NO and the formation of NO_2 vs. reaction time. On pure TiO_2, the NO concentration dropped rapidly at the beginning after turning on UV light, but NO increased shortly after a period of the reaction. The NO concentration monotonically increased even after 700 min of reaction. This phenomenon indicated NO was mainly undergoing oxidation on TiO_2 [33,34]. Even with propane available, NO was continuously oxidized to nitrite and nitrate, which occupied the catalyst surface leaving less sites for adsorption and eventually the catalyst would be saturated. Consequently, no more NO can be removed by TiO_2. On the other hand, when PtO_xPdO_y/TiO_2 was applied, a steady-state concentration of NO near 120 ppmv was reached after turning on UV light and

Table 1
Performance on photocatalytic NO reduction on various catalysts under UV light irradiation.

Catalyst	TiO_2	PdO_y/TiO_2	PtO_x/TiO_2	PtO_xPdO_y/TiO_2
Conversion (%)	60.3	63.3	62.5	69.5

Reaction condition: NO/C_3H_8 = 1/12, retention time = 19 min, UV-A light intensity = 46.9 mW/cm^2, reaction time = 4 h.

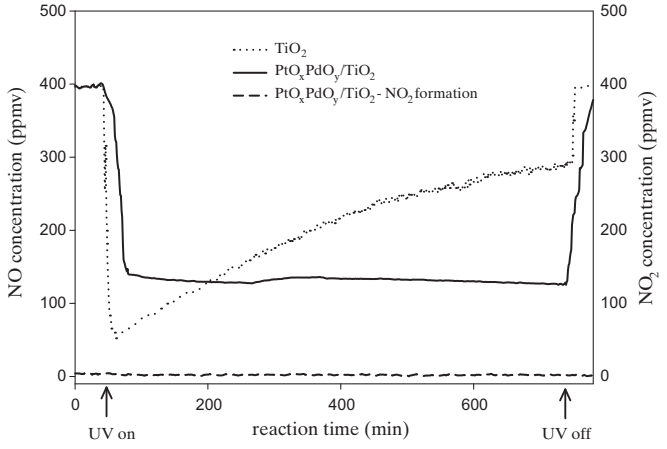

Fig. 4. NO concentrations vs. time on TiO_2 and PtO_xPdO_y/TiO_2 and the NO_2 formation vs. time on PtO_xPdO_y/TiO_2 in NO/C_3H_8 system. The NO concentration was back calculated to the corresponding concentration of the feed NO stream (i.e. 400 ppm in N_2) by the flow ratio of NO-feed-flow/total-flow rates.

throughout the whole reaction period. The NO_2 formation throughout the reaction was negligible. This clearly indicated that NO can be photocatalytically reduced to nitrogen on the PtO_xPdO_y/TiO_2 by propane, not only NO oxidation as in TiO_2. So all following experiments were carried out on PtO_xPdO_y/TiO_2.

Fig. 5 shows the performance comparison of monolith and powder-form photo reactors. The NO conversion in the monolith photo reactor was 15–20% higher than the simple plat-type reactor. The monolith photo reactor has a much larger contact area for heterogeneous catalysis and should show a significant increase in the NO conversion. However, due to the reactor design, UV light is guided only via the optical fibers. With the same UV light source, the light intensity per catalyst area of the monolith photo reactor actually was much less than that of the powder-form reactor. Therefore, the performance of the monolith photo reactor is, in fact, much better than the powder-form reactor.

Fig. 6 shows the NO conversion of the NO/propane system at three reaction temperatures. Reaction temperature was controlled at 25 °C, 70 °C, and 120 °C. The NO conversion was almost identical at 25 °C and 70 °C of about 90%. But at 70 °C, the rate increased so that the steady-state conversion reached 90% faster

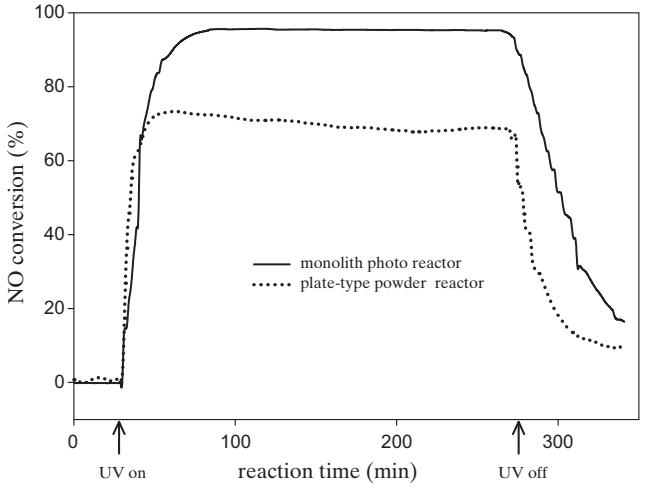

Fig. 5. Performance comparison of NO conversions in monolith and powder-form photoreactors with 0.5 g PtO_xPdO_y/TiO_2 in NO/C_3H_8 system under UV irradiation (molar ratio of NO:propane = 1:2500, retention time = 19 min, UV intensity = 46.9 mW/cm^2).

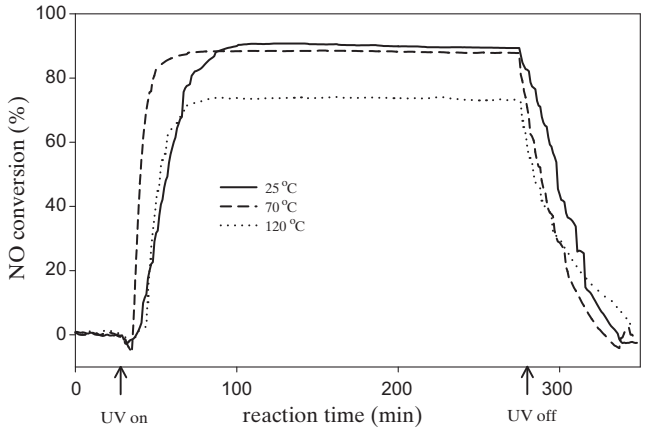

Fig. 6. NO conversion of NO/propane system using PtO_xPdO_y/TiO_2 as catalyst under UV irradiation at three reaction temperatures (molar ratio of NO:propane = 1:24, retention time = 19 min).

than that of 25 °C. A slight decrease of NO conversion to 73.1% was observed when temperature increased to 120 °C. Several phenomena of increasing reaction temperature of photocatalysis were reported in literatures [5,13,16,35–37]. In photocatalytic oxidation (PCO) processes, the reaction rate is usually temperature independent. The effect of reaction temperature mainly correlates to the adsorption–desorption process. When the reaction temperature increases, the adsorption ability of gaseous species on the catalyst surface will decrease and so does the conversion. However, in PCO processes, stable intermediates will form on the catalyst surface, increasing reaction temperature may promote desorption of stable intermediates attached on the catalyst surface, releasing the intermediate-occupied sites, therefore increasing the conversion. The decrease in NO conversion is the result of higher kinetic energy of gaseous molecules and lower adsorption density of reactants on the catalyst surface at higher temperature, as previously mentioned. In summary, raising the reaction temperature from 25 to 70 °C would slightly decrease the steady conversion but increase the rate. When the reaction temperature is further raised to 120 °C, the decrease in adsorption ability becomes dominant resulting in a lower conversion.

In the O_2 introduced system, the ratio of NO, C_3H_8, and O_2 are 1:24:120. Compare with the NO/propane system, the NO conversion decreased to 40.6% at room temperature as shown in Fig. 7. The decrease in NO conversion at 25 °C is due to the competition between NO and O_2 for photo generated electrons. The initial NO conversion at 70 °C is near 55.6% but the final steady-state conversion is very close to 25 °C. Unlike the NO/propane system, NO conversion reached 67.1% as temperature increased to 120 °C. Although not shown, NO_2 formation was negligible at 25 °C and 120 °C, but was observable near 20 ppm in the early stage of the reaction at 70 °C. At 70 °C, the steady-state conversion was very close to 25 °C as in the NO/propane system. The additional conversion was attributed to a fraction of NO that was oxidized to NO_2. Although PtO_xPdO_y/TiO_2 tends to reduce NO on the surface, large amount of adsorbed oxygen presented and the higher reaction rate at 70 °C would cause a fraction of NO to be oxidized, forming NO_2 at early stages of the reaction. As the reaction proceeded, NO conversion gradually returned to the steady state and the formation of NO_2 also decreased. When temperature increased to 120 °C, the NO conversion increased significantly while NO_2 formation decreased. This implies more NO was reduced and less was oxidized. This different trend of the temperature effects with respect to the simple NO/C_3H_8 system is due to the competition between O_2 and NO to capture the photo-generated electrons on the catalyst surface. Since NO is a polarized molecule and O_2 is not, the partially neg-

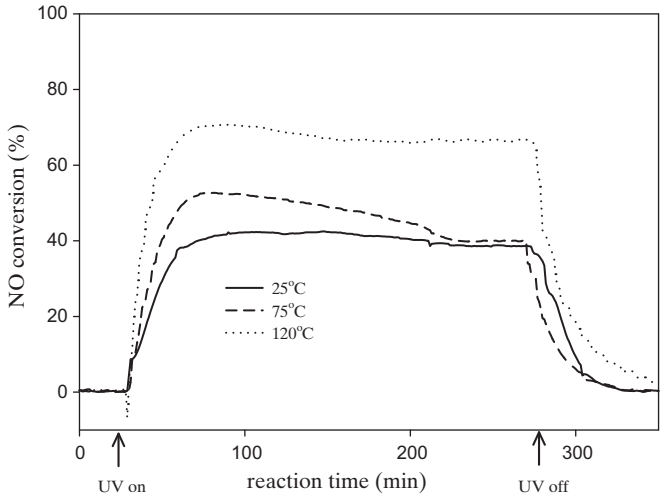

Fig. 7. NO conversion of NO/propane/O_2 system using PtO_xPdO_y/TiO_2 as catalyst under UV irradiation at three reaction temperatures (molar ratio of NO:propane:O_2 = 1:24:120, retention time = 19 min).

ative O atom on NO has a stronger affinity to the Ti^{4+} site, where the photo-generated electrons migrate to [38]. When temperature increases to 120 °C, both adsorbed NO and O_2 decreases. However, with much stronger adsorption ability, the fraction of NO adsorbed on the catalyst surface is higher resulting in a higher conversion near 73% as in the NO/C_3H_8 system.

Fig. 8 shows the NO conversions of the water vapor introduced system at three temperatures, respectively. The molar ratio between NO, propane, and water vapor is 1:24:41. The NO conversion significantly increased when temperature increased to 120 °C. The amount of water vapor added, compare with oxygen in the previous system is about 3:1. However, the NO conversions of the two systems were somewhat comparable. This indicates that water had a significant influence on adsorption rather than reaction. It is well known that TiO_2 becomes super hydrophilic under UV irradiation, since our system operates at relatively high humidity, a considerable amount of water molecules would adsorb strongly on the catalyst surface at 25 °C. When the temperature increases to 120 °C, large amount of water molecules would desorb, releasing the active sites from the catalyst surface. However, the adsorption ability of propane and NO do not change as much as water in this

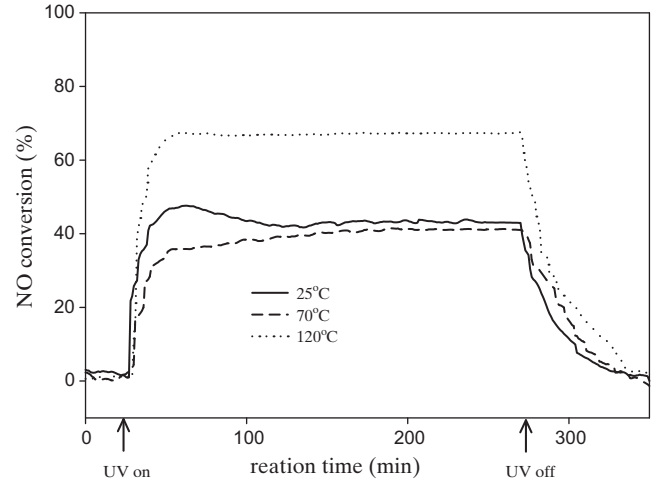

Fig. 8. NO conversion of NO/propane/H_2O system using PtO_xPdO_y/TiO_2 as catalyst under UV irradiation at three reaction temperatures (molar ratio of NO:propane:H_2O = 1:24:41, retention time = 19 min).

Table 2
Propane conversion of NO/propane/O_2 system.

Reaction temperature (°C)	NO/propane/O_2 (%)
25	40.0
70	27.3
120	10.0

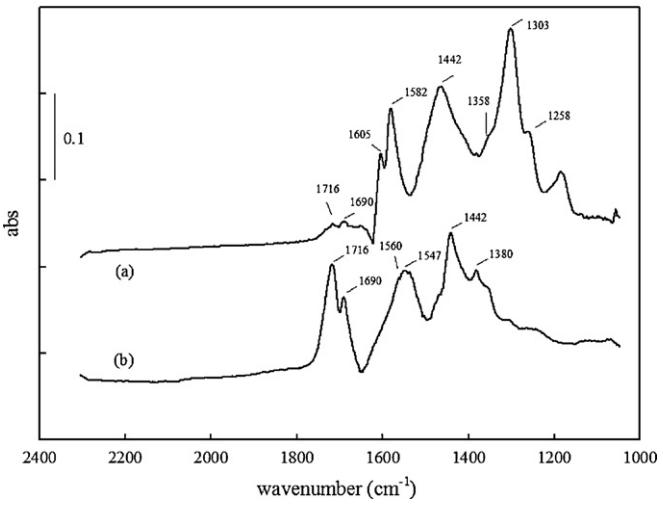

Fig. 9. In situ FTIR spectra of (a) TiO_2, (b) PtO_xPdO_y/TiO_2 under UV irradiation for NO/propane system (molar ratio of NO:propane = 1:24, reaction time = 19 min).

temperature range, resulting in the increase in the ratio of adsorbed NO and propane, thus increasing the NO conversion at elevated temperature.

A large number of hydrocarbon intermediates, such as acetone or formic acid, may be formed on the TiO_2 surface and occupy the sites. These intermediates may desorb by increasing temperature to 120 °C thus more vacant sites are available for the reaction. However, propane conversion decreased as temperature increased shown in Table 2. This indicates that increasing reaction temperature to 120 °C would decrease the adsorption of propane rather than enhance the desorption of intermediates. It should also be noted that from the GC analysis, only trace amount of acetone, acetaldehyde, or other hydrocarbon products were detected in the gas phase. This indicates hydrocarbon intermediates formed on the catalyst surface may not desorb. Further evidence is provided in the FTIR results.

Fig. 9 is the in situ FTIR spectra of the NO/propane reaction with TiO_2 and PtO_xPdO_y/TiO_2 as the photocatalysts. The wavenumbers related to each species are tabulated in Table 3. The FTIR spectra after 19 min of illumination were chosen to mimic the retention

Table 3
Assigned peak in NO/C_3H_8 and NO/C_3H_8/O_2 systems on PtO_xPdO_y/TiO_2 catalyst.

Peak (cm^{-1})	Species	Reference
1258	Bidentate nitrate	[46]
1303	Monodentate nitrate	[46]
1358	Formate	[47–49]
1380	Formate	[48,49]
1442	Acetate	[50,51]
1560	Formate	[49]
1582	Monodentate nitrate	[46]
1605	Bidentate nitrate	[46]
1690	Acetone	[14,47,52,53]
1716	Acetaldehyde	[53–55]
2235	N_2O	[45]
2341–2365	CO_2	[56]
2873	Formate	[47,53,56,57]
2952	Formate	[47,49,57]

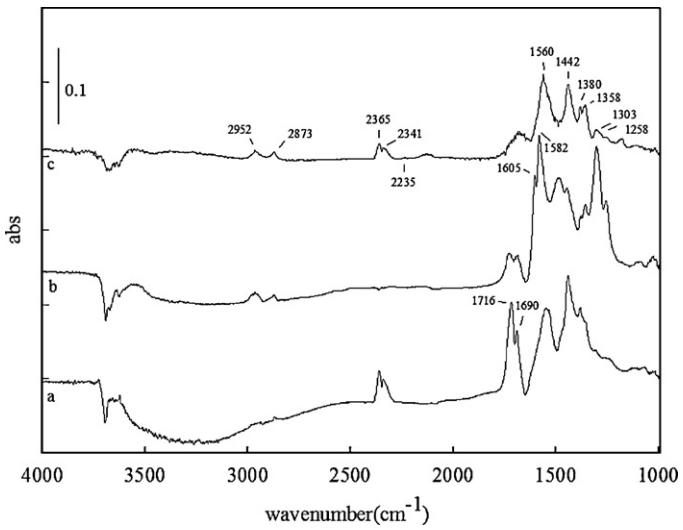

Fig. 10. In situ FTIR spectra of PtO_xPdO_y/TiO_2 under UV irradiation for NO/propane system at three reaction temperatures. (a) 25 °C, (b) 70 °C, (c) 120°C (molar ratio of NO:propane = 1:24, reaction time = 19 min).

time of the monolith reactor. Two spectra were identical above 2200 cm^{-1} so the absorption bands are shown only in the range from 1000 cm^{-1} to 2200 cm^{-1}. From Fig. 9, the surface species on TiO_2 were mainly products of NO oxidation. The peaks at 1303 and 1582 cm^{-1} correspond to monodentate nitrate and the peaks at 1258 and 1605 cm^{-1} refer to bidentate nitrate. On the other hand, the surface species on PtO_xPdO_y/TiO_2 are mainly products of C_3H_8 oxidation such as formate (1358, 1380, 1560 cm^{-1}), acetate (1442 cm^{-1}), acetone (1690 cm^{-1}), and acetaldehyde (1716 cm^{-1}). When applying PtO_xPdO_y/TiO_2, the peaks of nitrate (1258, 1303, 1605 cm^{-1}), which are strong on pure TiO_2, become shoulders or even diminish on the spectra. This clearly indicates that NO would tend to be reduced on the PtO_xPdO_y/TiO_2 catalyst surface. It is also consistent with the result as shown in Fig. 4.

Figs. 10 and 11 are the FTIR spectra of the NO/propane and NO/propane/O_2 systems at three reaction temperatures, respectively. From Fig. 10, various hydrocarbon species where identified such as formate (1358, 1380, 1560, 2873, 2952 cm^{-1}), acetate (1442 cm^{-1}), acetone (1690 cm^{-1}), acetaldehyde (1716 cm^{-1}), and

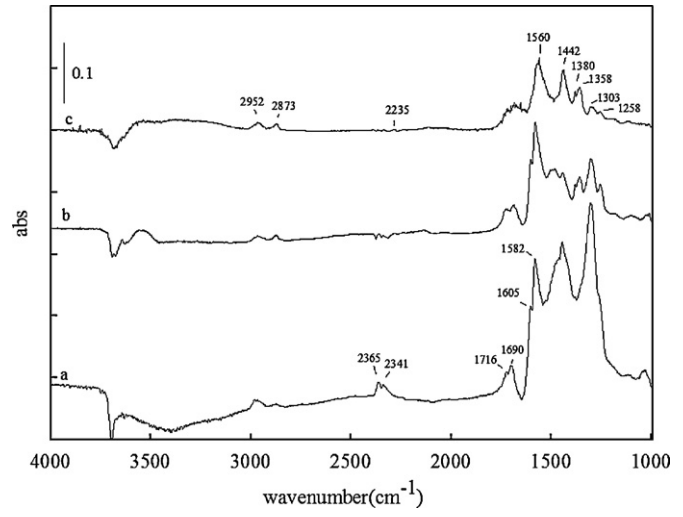

Fig. 11. In situ FTIR spectra of PtO_xPdO_y/TiO_2 under UV irradiation for NO/propane/O_2 systems at three reaction temperatures. (a) 25 °C, (b) 70 °C, (c) 120 °C (molar ratio of NO:propane:O_2 = 1:24:120, reaction time = 19 min).

the double signals between 2341 and 2365 cm^{-1} are related to the weak adsorption of carbon dioxide. Acetone, acetaldehyde, acetate and formate are the common products or intermediates in the propane or other hydrocarbon photocatalytic oxidation with molecular oxygen [39–42]. In this study, NO is the only oxidizing agent for propane oxidation on the catalyst surface. As a consequence, we expect NO to play the same role as O_2 in the oxidation path of C_3H_8. This indicates the oxidation of propane with NO is a step-by-step process and the ultimate product is CO_2. The signals at 1303 and 1582 cm^{-1} correspond to monodentate nitrate and the signals at 1258 and 1605 cm^{-1} refer to bidentate nitrate groups, which were inevitably formed. Nitrate and nitrite species are common products for the photocatalytic oxidation of NO [43,44]. Therefore, NO undergoes both oxidation and reduction with C_3H_8 presented.

While the temperature increases to 70 or 120 °C, almost all peaks in the spectra show identical position but different intensities. At 70 °C, the adsorbed amount of NO and propane were similar to 25 °C. However, due to a higher reaction rate, more nitrate and nitrite were formed at 70 °C. The higher reaction rate also caused adsorbed propane to oxidize further into formate or acetate. Once the temperature further increased to 120 °C, the peaks at 1605 and 1582 assigned as nitrate and nitrite are almost invisible. These peaks could be overlapped by the nearby hydrocarbon peaks and indicate less nitrate and nitrite formed on the surface. Another tiny but notable peak is observed around 2235 cm^{-1} in Fig. 10, which is assigned as N_2O in the literature [45]. Generally, N_2O could be the product or intermediate in the SCR process indicating another reduction path of NO. These phenomena could be contributed from the selectiveness of NO reaction path change with temperature.

The amount of O_2 was 120 times higher than that of NO, and O_2 served as the main oxidizing agent causing an increase in oxidation products such as nitrate, nitrite, and hydrocarbon intermediates. The magnitude of signals for nitrate, nitrite, and hydrocarbon intermediates in Fig. 11 were much higher than in Fig. 10. With an abundant source of oxygen, most propane was further oxidized to formate or acetate. As temperature rose from 25 °C to 120 °C, the signals referring to oxidation products decreased rapidly as shown in Fig. 11. This suggests that the adsorption of oxygen is relatively sensitive to temperature variations. As temperature rises, less O_2 are adsorbed and less nitrate, nitrite, and hydrocarbon intermediates are formed. However, the NO conversion still increased from near 40% to around 70% as temperature increased from 25 to 120 °C as shown in Fig. 7.

Fig. 12 is the FTIR spectra of the NO/propane/O_2 system at 120 °C after UV light was turned off. After the reaction was terminated, helium was purged continuously in order to remove the reacting species in the gas phase. Under this situation, the desorption of surface species should be enhanced due to the concentration gradient over the catalyst surface and gas phase at high temperature. However, the shape and magnitude of FTIR signals was almost identical from 5 to 20 min. This revealed that the surface species were intact, and raising reaction temperature to 120 °C was insufficient to overcome the binding of the chemisorbed intermediate species, whether there were nitrite/nitrate or hydrocarbon intermediates formed on the catalyst surface. As consistent with the GC analysis in the experiment, no desorption of hydrocarbon intermediates or nitrite/nitrate would occur from the catalyst surface under 120 °C. Thus the total amount of nitrite and nitrate can be estimated by dissolving in water after reaction using the ion chromatograph.

The potential products of NO photoreaction include N_2, N_2O, NO^-, NO_2, and NO_3^-. Based to the observed facts, we can conclude that (1) NO conversion increased while nitrate formation decreased with increasing reaction temperatures, and (2) nitrite and nitrate would not desorb under 120 °C and no NO_2 was observed. Although large amount of O_2 increased the driving force of NO oxidation, NO

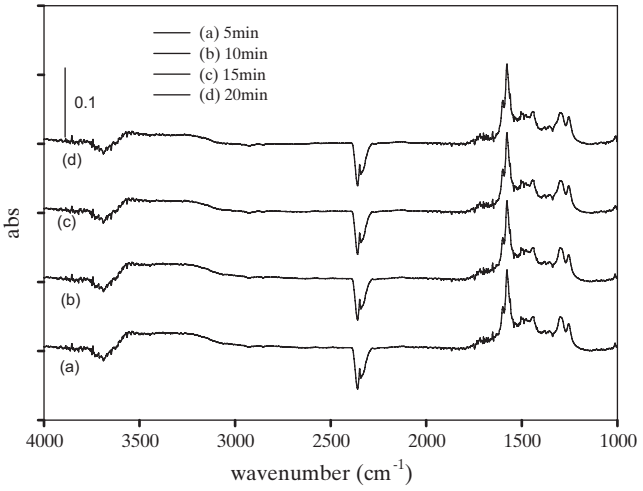

Fig. 12. In situ FTIR spectra of PtO_xPdO_y/TiO_2 for NO/propane/O_2 system after the photoreaction was over under UV off, helium purging conditions at 120 °C.

still had a high selectivity towards N_2 due to its stronger adsorption ability than O_2 at higher temperatures. In other words, the system is approximating the NO/propane system as temperature increases.

4. Conclusion

The PtO_xPdO_y/TiO_2 catalyst showed a very good performance of NO photoreduction while pure TiO_2 only gave NO oxidation using propane as a reducing agent. The photocatalytic reduction of NO achieved nearly 90% NO conversion on PtO_xPdO_y/TiO_2 at 25 °C. Raising reaction temperature to 70 °C decreased the conversion slightly but accelerated the speed to reach steady-state NO conversion. The conversion decreased to 73.1% as the reaction temperature increased to 120 °C due to the poor NO and propane adsorption. For the NO photoreaction with oxygen, oxygen competed with NO for photo-generated electrons leading to a low NO conversion at 25 °C. The NO conversion increased while the amount of surface formed nitrate decreased with temperature indicated that a high selectivity of NO converted towards N_2 at higher temperatures. Water vapor played a significant role not in reaction but rather in adsorption. When temperature rose to 120 °C, the adsorbed water on the TiO_2 surface desorbed considerably and a significant increase in NO conversion was observed. The oxidation products of NO and propane formed on the catalyst surface were observed by in situ FTIR spectroscopy. The results of FTIR revealed that temperature variations might affect on reaction paths.

Acknowledgements

The authors acknowledge the financial support from the National Science Council of Taiwan under contract NSC 98-2911-I-002-002 and the Ministry of Economic Affairs of Taiwan under grant 97-EC-17-A-09-S1-019.

References

[1] R. Burch, J.P. Breen, F.C. Meunier, Appl. Catal. B: Environ. 39 (2002) 283–303.
[2] S. Roy, M.S. Hegde, G. Madras, Appl. Energy 86 (2009) 2283–2297.
[3] N. Serpone, E. Pelizzetti, Photocatalysis: Fundamentals and Applications, Wiley, New York, 1989.
[4] A. Fujishima, K. Honda, Nature 238 (1972) 37–38.
[5] J. Zhang, T. Ayusawa, M. Minagawa, K. Kinugawa, H. Yamashita, M. Matsuoka, M. Anpo, J. Catal. 198 (2001) 1–8.
[6] T. Tanaka, K. Teramura, T. Yamamoto, S. Takenaka, S. Yoshida, T. Funabiki, J. Photochem. Photobiol. A 148 (2002) 277–281.
[7] K. Teramura, T. Tanaka, S. Yamazoe, K. Arakaki, T. Funabiki, Appl. Catal. B: Environ. 53 (2004) 29–36.
[8] S. Yamazoe, T. Okumura, K. Teramura, T. Tanaka, Catal. Today 111 (2006) 266–270.
[9] S. Roy, M.S. Hegde, N. Ravishankar, G. Madras, J. Phys. Chem. C 111 (2007) 8153–8160.
[10] S. Yamazoe, K. Teramura, Y. Hitomi, T. Shishido, T. Tanaka, J. Phys. Chem. C 111 (2007) 14189–14197.
[11] A. Fritz, V. Pitchon, Appl. Catal. B: Environ. 13 (1997) 1–25.
[12] V.I. Pârvulescu, P. Grange, B. Delmon, Catal. Today 46 (1998) 233–316.
[13] T.M. Twesme, D.T. Tompkins, M.A. Anderson, T.W. Root, Appl. Catal. B: Environ. 64 (2006) 153–160.
[14] T. van der Meulen, A. Mattson, L. Österlund, J. Catal. 251 (2007) 131–144.
[15] N. Bouazza, M.A. Lillo-Ródenas, A. Linares-Solano, Appl. Catal. B: Environ. 84 (2008) 691–698.
[16] T.H. Lim, S.M. Jeong, S.D. Kim, J. Gyenis, J. Photochem. Photobiol. A 134 (2000) 209–217.
[17] S. Poulston, M.V. Twigg, A.P. Walker, Appl. Catal. B: Environ. 89 (2009) 335–341.
[18] J. Araña, J.M. Doña-Rodríguez, O. González-Díaz, E. Tello Rendón, J.A. Herrera Melián, G. Colón, J.A. Navío, J. Pérez Peña, J. Mol. Catal. A: Chem. 215 (2004) 153–160.
[19] C.-H. Lin, J.-H. Chao, C.-H. Liu, J.-C. Chang, F.-C. Wang, Langmuir 24 (2008) 9907–9915.
[20] J. Mo, Y. Zhang, Q. Xu, J.J. Lamson, R. Zhao, Atmos. Environ. 43 (2009) 2229–2246.
[21] M.L. Sauer, D.F. Ollis, J. Catal. 149 (1994) 81–91.
[22] J. Blanco, P. Avila, S. Suarez, M. Yates, J.A. Martin, L. Marzo, C. Knapp, Chem. Eng. J. 97 (2004) 1–9.
[23] P. Avila, M. Montes, E. Miró Eduardo, Chem. Eng. J. 109 (2005) 11–36.
[24] P. Du, J.T. Carneiro, J.A. Moulijn, G. Mul, Appl. Catal. A: Gen. 334 (2008) 119–128.
[25] J.T. Carneiro, R. Berger, J.A. Moulijn, G. Mul, Catal. Today 147 (2009) S324–S329.
[26] C. Nicolella, M. Rovatti, Chem. Eng. J. 69 (1998) 119–126.
[27] M.M. Hossain, G.B. Raupp, S.O. Hay, T.N. Obee, AIChE J. 45 (1999) 1309–1321.
[28] M. Moazzem Hossain, G.B. Raupp, Chem. Eng. Sci. 54 (1999) 3027–3034.
[29] M. Singh, I. Salvadó-Estivill, G.L. Puma, AIChE J. 53 (2007) 678–686.
[30] M. Ren, K.T. Valsaraj, Sep. Purif. Technol. 62 (2008) 523–528.
[31] S.J. Limmer, S. Seraji, Y. Wu, T.P. Chou, C. Nguyen, G.Z. Cao, Adv. Funct. Mater. 12 (2002) 59–64.
[32] J.C.S. Wu, Y.-T. Cheng, J. Catal. 237 (2006) 393–404.
[33] K. Hashimoto, K. Wasada, M. Osaki, E. Shono, K. Adachi, N. Toukai, H. Kominami, Y. Kera, Appl. Catal. B: Environ. 30 (2001) 429–436.
[34] M.M. Ballari, M. Hunger, G. Hüsken, H.J.H. Brouwers, Appl. Catal. B: Environ. 95 (2010) 245–254.
[35] X. Fu, L.A. Clark, W.A. Zeltner, M.A. Anderson, J. Photochem. Photobiol. A 97 (1996) 181–186.
[36] S.B. Kim, H.T. Hwang, S.C. Hong, Chemosphere 48 (2002) 437–444.
[37] M.J. Backes, A.C. Lukaski, D.S. Muggli, Appl. Catal. B: Environ. 61 (2005) 21–35.
[38] M. Takeuchi, J. Deguchi, S. Sakai, M. Anpo, Appl. Catal. B: Environ. 96 (2010) 218–223.
[39] N. Djeghri, M. Formenti, F. Juillet, S.J. Teichner, Faraday Discuss. Chem. Soc. 58 (1974) 185–193.
[40] C. Hagglund, B. Kasemo, L. Osterlund, J. Phys. Chem. B 109 (2005) 10886–10895.
[41] J. Araña, J.M. Doña-Rodríguez, J.A.H. Melián, E.T. Rendón, O.G. Díaz, J. Photochem. Photobiol. A 174 (2005) 7–14.
[42] J. Araña, A.P. Alonso, J.M.D. Rodríguez, G. Colón, J.A. Navío, J.P. Peña, Appl. Catal. B: Environ. 89 (2009) 204–213.
[43] S. Devahasdin, C. Fan, K. Li, D.H. Chen, J. Photochem. Photobiol. A 156 (2003) 161–170.
[44] Y.-H. Tseng, C.-S. Kuo, C.-H. Huang, Y.-Y. Li, P.-W. Chou, C.-L. Cheng, M.-S. Wong, Nanotechnology 17 (2006) 2490.
[45] F. Poignant, J.L. Freysz, M. Daturi, J. Saussey, Catal. Today 70 (2001) 197–211.
[46] L. Li, Q. Shen, J. Cheng, Z. Hao, Catal. Today 158 (3–4) (2010) 361–369.
[47] A. Mattsson, M. Leideborg, K. Larsson, G. Westin, L. Osterlund, J. Phys. Chem. B 110 (2005) 1210–1220.
[48] F. Boccuzzi, A. Chiorino, M. Manzoli, J. Power Sources 118 (2003) 304–310.
[49] G. Busca, J. Lamotte, J.C. Lavalley, V. Lorenzelli, J. Am. Chem. Soc. 109 (1987) 5197–5202.
[50] Z. Yu, S.S.C. Chuang, J. Catal. 246 (2007) 118–126.
[51] L.-F. Liao, W.-C. Wu, C.-Y. Chen, J.-L. Lin, J. Phys. Chem. B 105 (2001) 7678–7685.
[52] M.D. Hernández-Alonso, I. Tejedor-Tejedor, J.M. Coronado, M.A. Anderson, J. Soria, Catal. Today 143 (2009) 364–373.
[53] J.M. Coronado, S. Kataoka, I. Tejedor-Tejedor, M.A. Anderson, J. Catal. 219 (2003) 219–230.
[54] J.E. Rekoske, M.A. Barteau, Langmuir 15 (1999) 2061–2070.
[55] C.-A. Chang, B. Ray, D.K. Paul, D. Demydov, K.J. Klabunde, J. Mol. Catal. A: Chem. 281 (2008) 99–106.
[56] M. El-Maazawi, A.N. Finken, A.B. Nair, V.H. Grassian, J. Catal. 191 (2000) 138–146.
[57] J. Raskó, T. Kecskés, J. Kiss, J. Catal. 224 (2004) 261–268.